Supporting Information:

Cell Membrane-Anchored Biosensors for Real-Time Monitoring of the Cellular Microenvironment

Liping Qiu, [†, ‡] Tao Zhang, [‡] Jianhui Jiang, [†,*] Cuichen Wu, [‡] Guizhi Zhu, [†,‡] Mingxu You, [†, ‡] Xigao Chen, [‡] Liqin Zhang, [‡] Cheng Cui, [‡] Ruqin Yu[†] and Weihong Tan[†,‡,*]

[†:] Molecular Science and Biomedicine Laboratory, State Key Laboratory of Chemo/Biosensing and Chemometrics, College of Chemistry and Chemical Engineering, College of Biology, Collaborative Innovation Center for Molecular Engineering for Theranostics, Hunan University, Changsha, 410082, China

[‡:] Center for Research at Bio/Nano Interface, Department of Chemistry and Department of Physiology and Functional Genomics, Shands Cancer Center, UF Genetics Institute and McKnight Brain Institute, University of Florida, Gainesville, Florida 32611-7200, United States

*Address correspondence to tan@chem.ufl.edu and jianhuijiang@hnu.edu.cn

Experimental Section

1. Probe Synthesis

The diacyllipid phosphoramidite was synthesized in two steps following the protocol of our previous report.[1] All oligonucleotide sequences were synthesized using an ABI 3400 DNA synthesizer (Applied Biosystems, Foster City, CA, USA) on a 1.0 micromole scale. Lipophilic phosphoramidites dissolved in dichloromethane were coupled onto the 5' ends of the oligonucleotides. After synthesis, oligonucleotides were deprotected and cleaved from the corresponding controlled pore glass (CPG) according to reagent instructions. Then, all oligonucleotides were precipitated by adding 3 M NaCl (1/10 volume) and cold ethanol (2.5-times volume). After having been frozen for 30 min, the precipitated oligonucleotides were collected by centrifugation, dissolved in 0.2 M triethylammonium acetate (TEAA, Glen Research Corp), and then purified by HPLC (ProStar, Varian, Walnut Creek, CA, USA) using acetonitrile and 0.2 M TEAA as the mobile phase. Oligonucleotides with and without diacyllipid were purified using a C4 column (BioBasic-4, 200mm x 4.6mm, Thermo Scientific) and a C18 column (5 μm, 250 mm ×4.6 mm, Alltech), respectively. Finally, these oligonucleotides were

quantified by measuring their 260-nm absorption with a UV-vis spectrometer (Cary Bio-300, Varian).

2. Cell Culture and Modification

CCRF-CEM cells (human acute lymphoblastic leukemia) were purchased from American Type Culture Collection and cultured in RPMI 1640 medium supplemented with 10% FBS (heat-inactivated; Gibco) and 0.5 mg/mL penicillin–streptomycin (Cellgro). For surface modification, cells (2.5×10^5) were washed three times with HEPES buffer (50 mM HEPES, pH 7.3, 270 mM NaCl) and incubated with lipid-DNA probes (1 μM) at room temperature (RT, 25 ^{o}C). An incubation time of 30 min was used, unless otherwise stated. Then, the cells were washed three times to remove free probes and resuspended in 180 μL HEPES buffer. For Mg^{2+} assays, 0.2 mM EDTA was added to the buffer solution to quench the Mg^{2+} released during the cell modification process.

3. Fluorescence kinetics detection

Fluorescence measurements were carried out on a FluoroMax-4 spectrofluorometer using the kinetics analysis mode with excitation at 488 nm and emission at 520 nm. For each experiment, lipid-DNAzyme and substrate were mixed in a 90-μL HEPES buffer solution (both concentrations were 200 nM), heated at 95 ^{o}C for 5 min, and then slowly cooled to RT to facilitate DNA hybridization. After transfer of the annealed mixture into a microcuvette, the fluorescence intensity was recorded at 10-s intervals, and 10 μL of specific metal ions at a certain concentration were then added to initiate the cleavage reaction.

4. Quantitation of Surface-Density of Diacyllipid-DNA Probe

CEM cells (1×10^7) were incubated with 1 μM diacyllipid-DNA-TAMRA at RT for different lengths of time, washed three times with HEPES buffer, and then lysed with 100 μL cell lysis buffer (10 mM Tris-HCl buffer containing 100 mM NaCl, 1 mM EDTA and 1% Triton X-100, pH 7.4). After that, TAMRA fluorescence was collected with a FluoroMax-4 spectrofluorometer.

The concentration of the DNA probe was calculated by fitting the detected fluorescence intensity to a standard curve.

5. Flow Cytometry and Confocal Laser Scanning Microscopy (CLSM) Assay

Flow cytometry was performed on a FACScan cytometer (Accuri C6) by counting 10000 events. To initiate the DNAzymatic reaction, 20 μL of target metal ion or stimulant at a certain concentration was added to the probe-modified cell mixture. Subsequently, the cells were subjected to flow cytometry at a given time point. The data were processed with FlowJo software.

CLSM measurements were conducted on a Leica TCS SP5 confocal microscope (Leica Microsystems) with a 40× oil-immersion objective. The probe-modified cells were treated with target metal ions or stimulants following the same procedure described above.

Table S1. DNA sequences designed in this work.

Note	Sequence (5'→ 3')
Mg-DNAzyme	Diacyllipid-PEG- CGA CGA CTC CTC T TC AGC GAT CCG GAA CGG CAC CCA TGT TAG TGA CCC-FITC/TAMRA)
Mg-Substrate	DABCYL- GGGTCACTAT rA GGAAGAGGAGTCGTCG
Pb-DNAzyme	Diacyllipid-PEG-GACACAGACATCATCTCTGAAGTAGCGCCGCCGTATAGTGAC-FITC
Pb-Substrate	DABCYL- GCTCACTATrAGGAAGAGATGACG
Zn-DNAzyme	CCTCCATCTCTTCT CCGAGCCGGTCGAA ATAGTGAGC-FITC
Zn-Substrate	DABCYL- GCTCACTAT rA GGAAGAGATGGAGG

Note: The length of each PEG molecule is ~1.8 nm.

Table S2. Quantification of surface density of diacyllipid-DNA-TAMRA probe

	15 min	30 min	60 min	90 min	120 min
Number of DNAs/cell	$1.31\pm0.14\times10^6$	$1.65\pm0.16\times10^6$	$1.71\pm0.14\times10^6$	$1.83\pm0.09\times10^6$	$1.89\pm0.18\times10^6$
Coverage*	1.31%	1.65%	1.71%	1.83%	1.89%

Note: * % coverage was estimated based on a cell diameter of 10 μm and a DNA probe diameter of 2 nm.

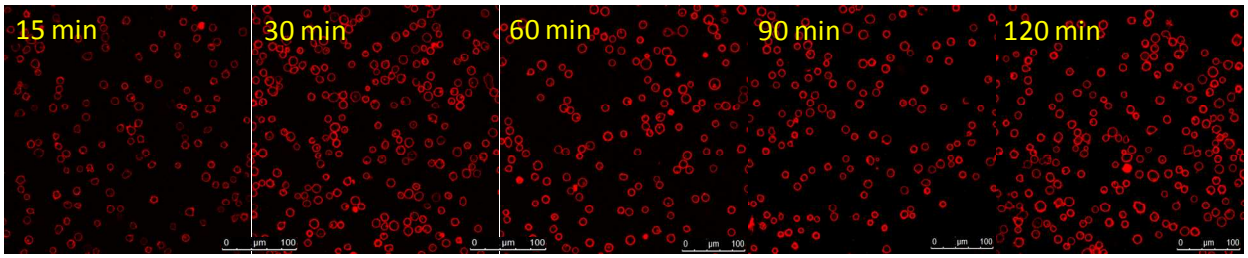

Figure S1. CLSM images of CEM cells incubated with 1 μM diacyllipid-DNA-TAMRA at RT for different lengths of time. Scale bar represents 50 μm.

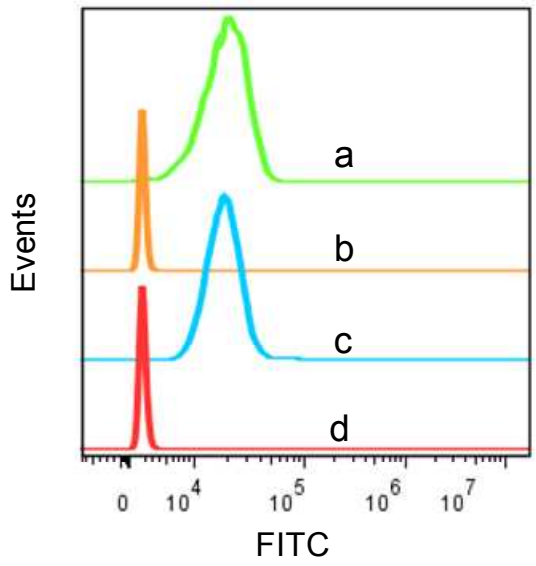

Figure S2. Flow assay of CEM cells incubated with the diacyllipid-DNA-FITC (curve a) or the diacyllipid-DNA-FITC/cDNA-DABCYL hybrid (curve b) at room temperature for 30 min; or CEM cells first incubated with the diacyllipid-DNA-FITC conjugate at room temperature for 30 min, washed by centrifugation, and then incubated with PBS (curve c) or the cDNA-DABCYL (curve d) for another 30 min.

The orientation of the DNA sensors on the cell membrane was investigated with the following experiment. First, the CEM cells were incubated with the diacyllipid-DNA-FITC conjugates at room temperature for 30 min. After removal of free DNA probes, the modified cells were incubated with the cDNA-DABCYL which is complementary to the DNA-FITC probe of the conjugate (curve d) for another 30 min. To get the maximum unquenched fluorescence signal, a control experiment was conducted by replacing the cDNA-DANCYL with the corresponding buffer solution (curve c). After removal of free cDNA-DABCYLs, the resultant cells were analyzed by flow cytometry. As shown in Figure S2, the fluorescence of the membrane-anchored DNA-FITC was obviously quenched resulting from the hybridization between the DNA-FITC probe and the cDNA-DABCYL (curve d). The reduction of fluorescence in this case is almost the same as that of the sample which was directly incubated with the diacyllipid-DNA-FITC/cDNA-DABCYL hybrid (curve b), indicating a complete hybridization between the membrane-immobilized DNA-FITC and the subsequently added cDNA-DABCYL. Since oligonucleotides are negatively charged hydrophilic macromolecules

and cannot freely permeate the lipophilic cell membrane, the cDNA-DABCYL can only hybridize the DNA probe on the extracellular side of the cell membrane. In other words, the DNA probes should mainly localize on the outer leaflet of the cell membrane.

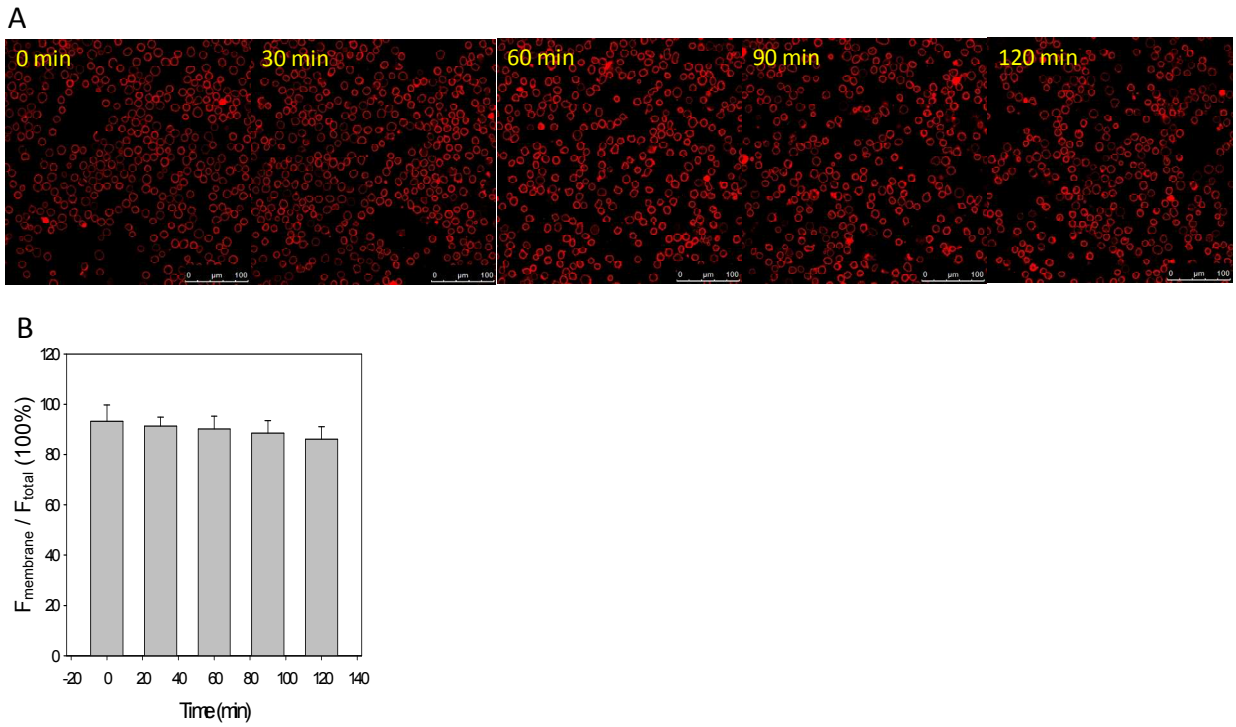

Figure S3. Cellular internalization level of diacyllipid-DNA conjugates at 37 ^{o}C. (A) CLSM images of CEM cells incubated with 1 μM diacyllipid-DNA-TAMRA at RT for 30 min, washed three times, and then held at 37 ^{o}C for different lengths of time. (B) The corresponding fluorescence signal ratio between the cell membranes ($F_{membrane}$) and the whole cells (F_{total}).

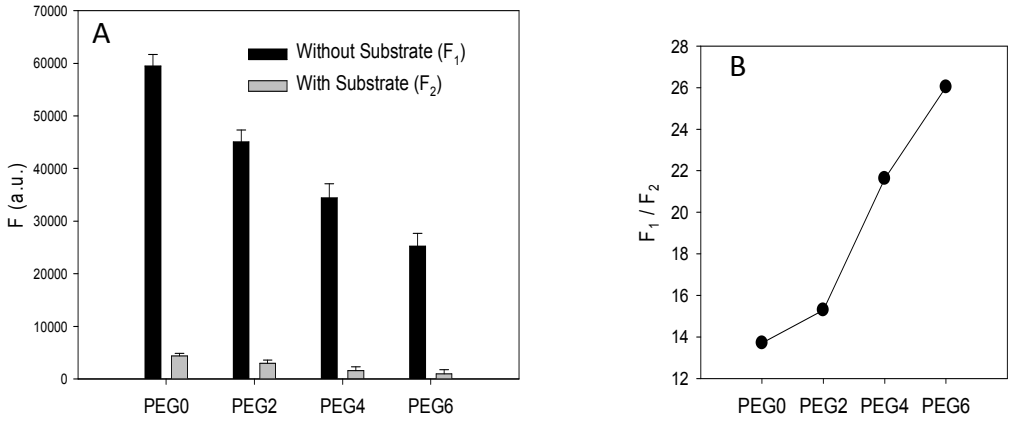

Figure S4. Optimization of PEG linker length. (A) Flow cytometry assay of CEM cells separately incubated with four diacyllipid-DNA-FITC probes (1 μM) having different lengths of PEG spacer (PEG0, PEG2, PEG4, and PEG6 represent 0, 2, 4, and 6 PEG molecules, respectively). The black bar and the gray bar represent the mean fluorescence signal of the cells treated with the diacyllipid-DNAzyme probe hybridized without (F_1) and with (F_2) substrate, respectively. Error bars represent the standard deviation of three independent experiments (B) The corresponding signal ratio was calculated by dividing F_1 by F_2.

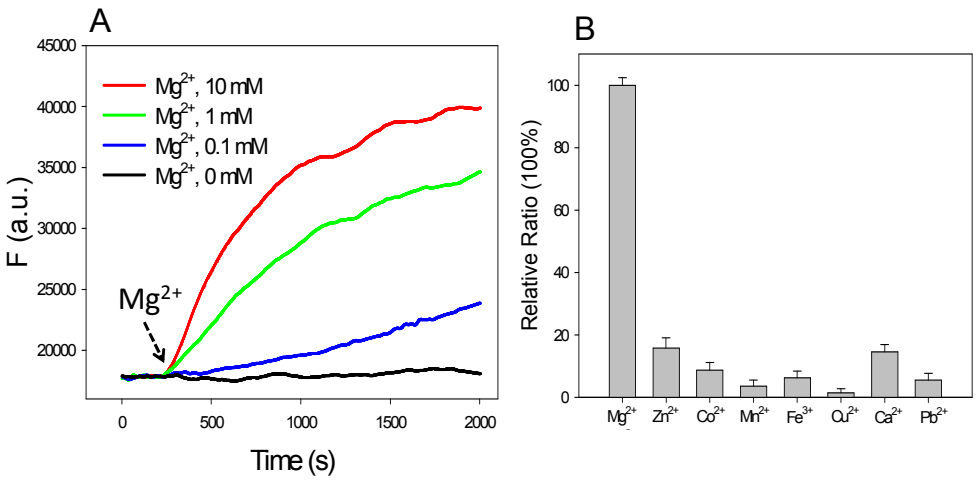

Figure S5. Performance of Mg-DNAzyme in buffer system. (A) Fluorescence kinetics spectroscopy of Mg-DNAzyme (200 nM) after injection of Mg^{2+} at different concentrations. (B) Selectivity of the Mg-DNAzyme. The concentrations of Mg^{2+} and other competing metal ions were 1 mM each. The signal in response to Mg^{2+} was defined as 100%, while the signals of other metal ions were calculated as the relative value. Error bars represent the standard deviation of three independent experiments.

As shown in Figure S4A, the fluorescence signal increased with increasing Mg^{2+} concentration from 0 to 10 mM. Further assays of this Mg-DNAzyme showed that the apparent dissociation constant (K_d) was 0.93 ± 0.13 mM (R^2= 0.998) and that the observed rate constant (k_{obs}) for 1 mM Mg^{2+} was 0.15 min^{-1} (R^2= 0.980). This k_{obs} value was 3 times higher than that of a previous report[2], mainly due to the enhanced duplex stability resulting from the extended complementary base pairs at the 5'-end of the DNAzyme, which facilitated the formation of the Mg^{2+} binding pockets (Table S1). In addition, the much weaker signal in response to other metal ions demonstrates the high selectivity of this DNAzyme (Figure S4B).

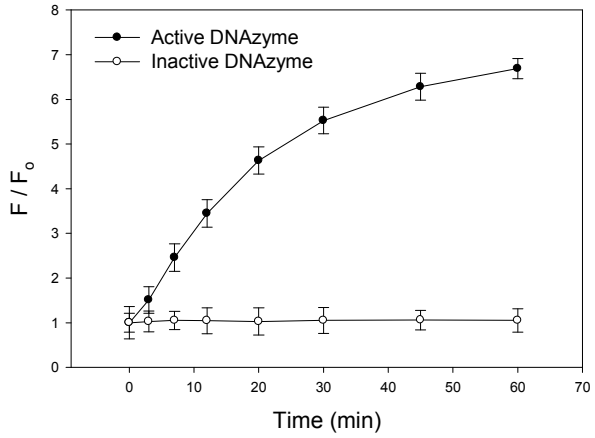

Figure S6. Flow kinetics assay of CEM cells modified with active Mg-DNAzyme and inactive Mg-DNAzyme (the rA in the substrate was replaced with a DNA nucleotide, A) after addition of 1 mM Mg^{2+}. Error bars represent the standard deviation of three independent experiments.

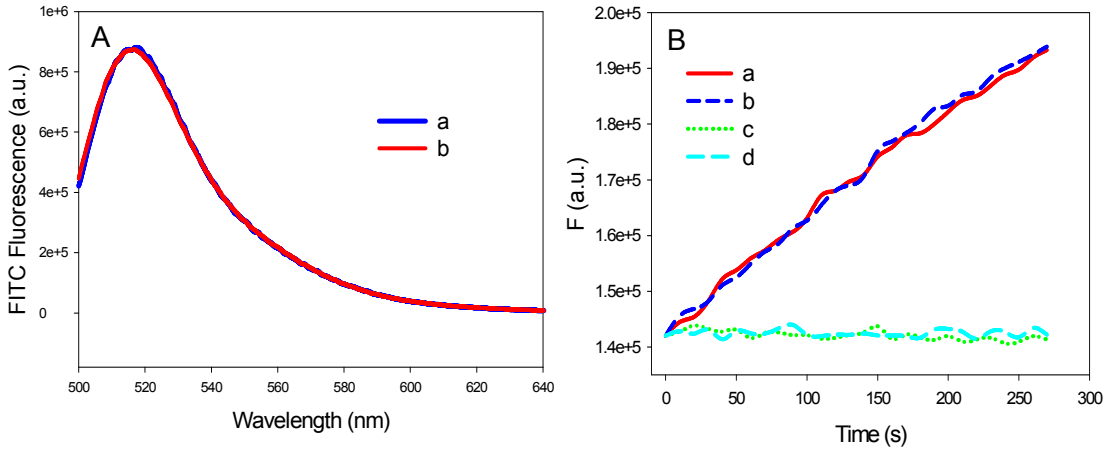

Figure S7. Negligible interference of α1-adrenoceptor on the fluorescence properties of FITC and cleavage activity of Mg-DNAzyme. (A) Fluorescence spectra of DNA-FITC without (curve a) and with (curve b) 0.5 mM α1-adrenoceptor. (B) Fluorescence kinetics spectroscopy of Mg-DNAzyme treated with 1 mM Mg^{2+} (curve a), with 1 mM Mg^{2+} plus 0.5 mM α1-adrenoceptor (curve b), buffer only (curve c), or with 0.5 mM α1-adrenoceptor (curve d).

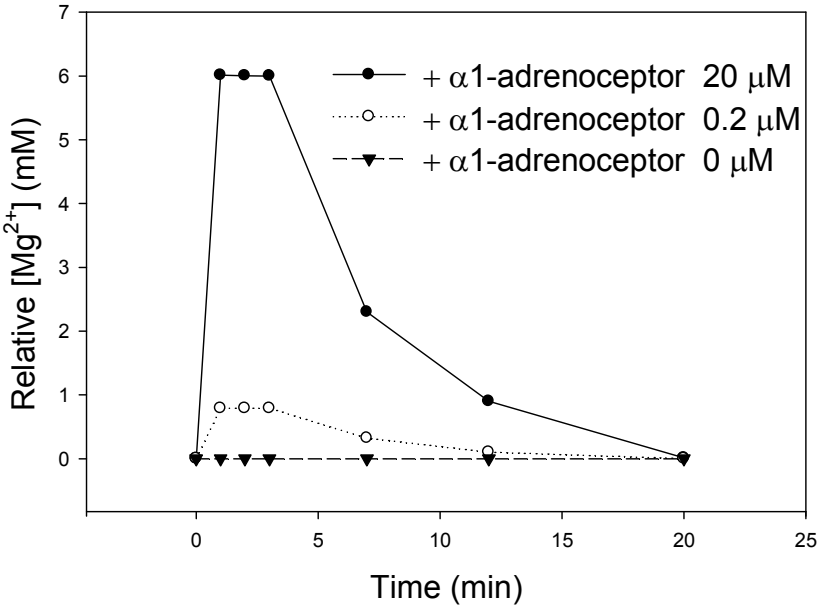

Figure S8. The time-dependent concentration profile revealing the dynamics of Mg^{2+} release for the cells stimulated by α1-adrenoceptor.

We could assume that the fluorescence activation rate of our membrane-anchored sensor at a specific moment during Mg^{2+} transport out of the cells equals to the initial rate of fluorescence activation in the case when the sensor was incubated with externally added Mg^{2+}, provided the concentration of the added Mg^{2+} is the same as that of the transported Mg^{2+}. This assumption enables us to calculate the relative instantaneous concentration of transported Mg^{2+} at a specific moment by using a calibration curve of initial fluorescence activation rates obtained via incubating the sensor with Mg^{2+} of varying concentrations. As shown in Figure 2A, the fluorescence signal increases almost linearly at the initial reaction period up to 12 min. So, we can calculate the initial fluorescence activation rates for different Mg^{2+} concentrations using the slopes of the fluorescence activation curves at the initial reaction period and obtain the calibration curve for initial fluorescence activation rate versus Mg^{2+} concentration. Assuming the concentrations of Mg^{2+} during its transport out of the cells does not vary abruptly (no substantial change in 3 min), the relative instantaneous concentration of transported Mg^{2+} at a specific moment can be calculated according to the fluorescence activation rate at this time point with reference to the calibration curve. Meanwhile, we can assume that the number of the anchored DNAzyme is much more than the amount of the released Mg^{2+}, which can be verified by the

much lower response signal compared with the maximum fluorescence. In this way, the relative instantaneous Mg^{2+}concentrations during its cross-membrane transport at different moments are obtained and plotted as a time-dependent profile. This time-dependent concentration profile thus reveal the dynamics of Mg^{2+} transport for cells stimulated by α1-adrenoceptor.

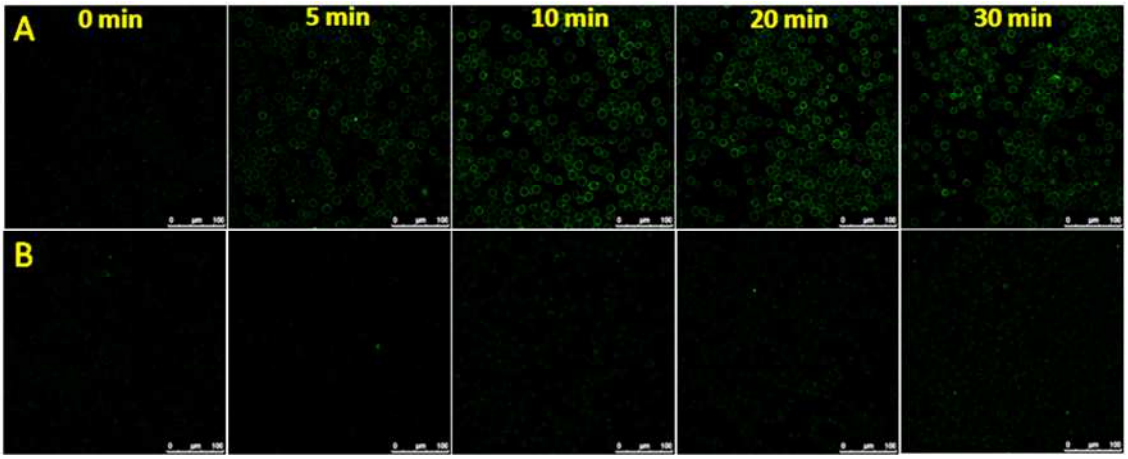

Figure S9. CLSM image of Mg-DNAzyme-modified cells treated with (A) and without (B) 20 μM α1-adrenoceptor at 37 ^{o}C for different lengths of time.

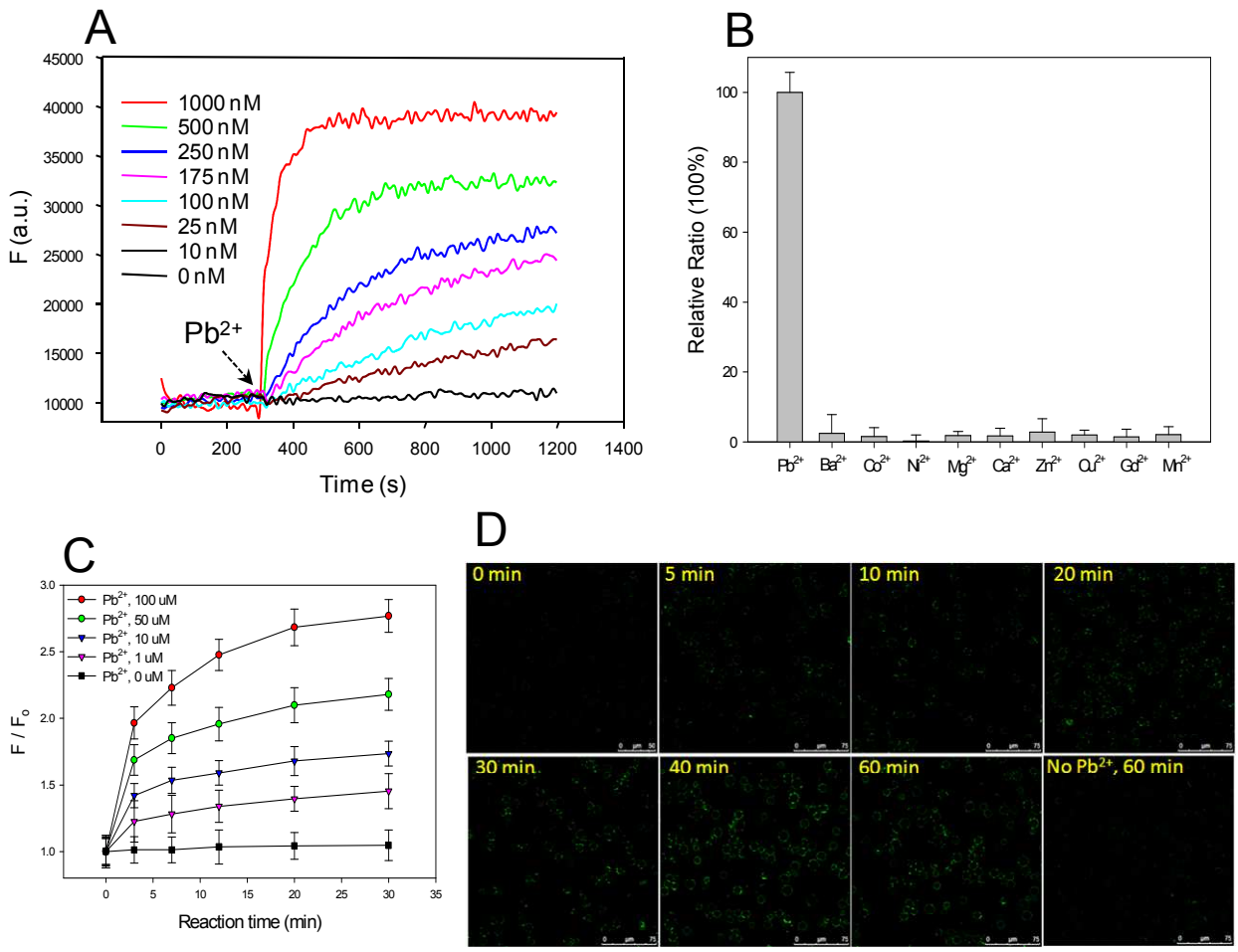

Figure S10. Universality of cell-surface DNAzyme system. (A) Fluorescence kinetics study of Pb-DNAzyme (200 nM) treated with Pb^{2+} at different concentrations. (B) Selectivity of the Pb-DNAzyme. The concentration of Pb^{2+} was 100 nM, and that of other competing metal ions was 100 μM. The signal in response to Pb^{2+} was defined as 100%, while that of other metal ions was calculated as the relative value. Error bars represent the standard deviation of three independent experiments. (C) Flow kinetics assay of the Pb-DNAzyme-modified CEM cells treated with different concentrations of Pb^{2+}. Error bars represent the standard deviation of three independent experiments. (D) CLSM images of the Pb-DNAzyme-modified CEM cells treated with Pb^{2+} (100 μM) for different time spans. Without addition of Pb^{2+}, no obvious FITC signal was observed, even after incubation for 60 min, compared with the pattern of gradual illumination of cells treated with 100 μM Pb^{2+}, demonstrating the excellent capacity of this cell-surface Pb-DNAzyme for signaling extracellular Pb^{2+}.

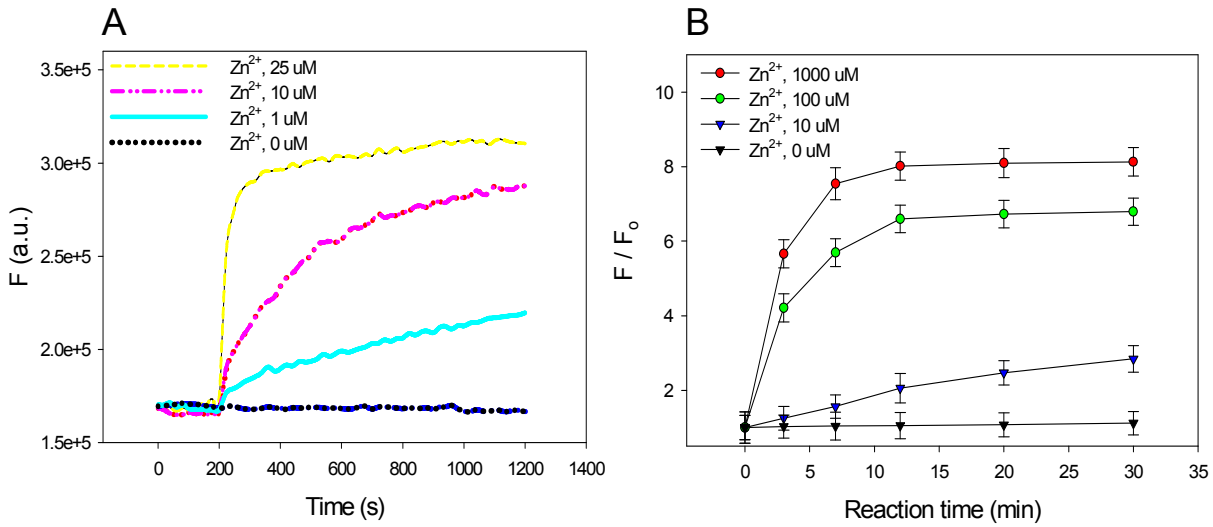

Figure S11. Performance of Zn-DNAzyme. (A) Fluorescence kinetics of Zn-DNAzyme (200 μM) in the presence of Zn^{2+} at different concentrations in buffer system. (B) Flow cytometry assay of cell-surface Zn-DNAzyme in the presence of Zn^{2+} at different concentrations. Error bars represent the standard deviation of three independent experiments.

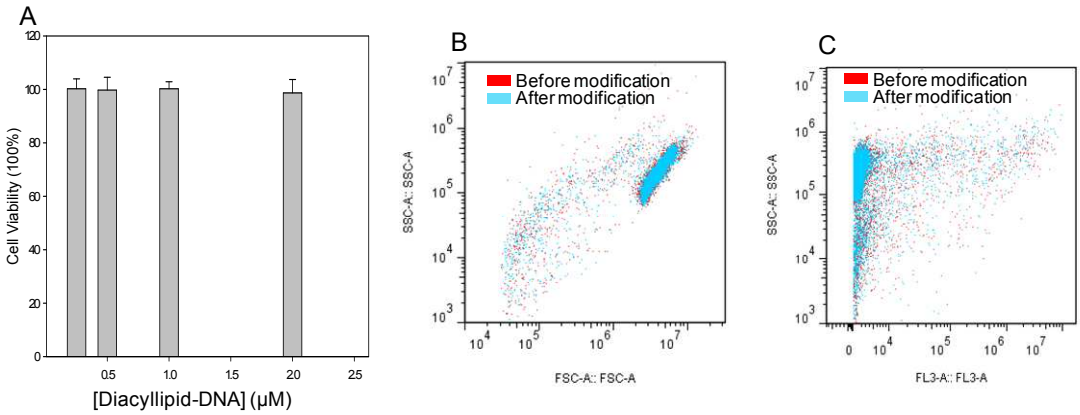

Figure S12. MTS assay of the CEM cells incubated with the diacyllipid-DNA conjugates of different concentrations (A). Flow assay (B) and PI staining test (C) of the CEM cells before and after incubation with 1 μM diacyllipid-DNA conjugates. All the incubation processes were performed at room temperature for 30 min.

MTS assay of cells with the diacyllipid-DNA conjugates inserted into the cell membrane. As the diacyllipid-DNA coverage is relatively small, the impact is limited. The results showed no observable difference of the cellular viability before and after membrane modification, demonstrating that the insertion of the diacyllipid-DNA conjugates into the cell membrane did not affect the cellular proliferation.

References:

（1）Wu, Y.; Sefah, K.; Liu, H.; Wang, R.; Tan, W. *Proc. Natl. Acad. Sci.* **2010**, *107*, 5.

(2) KiáLee, N.; RanáKoh, H.; YoungáHan, K.; KeunáKim, S. *Chem. Commun.* **2010**, *46*, 4683.